

SHEP 95-01

January 1995

Charginos and Neutralinos at LEP II

Marco A. Díaz and Steve F. King

*Physics Department, University of Southampton
Southampton, SO17 1BJ, U.K.*

Abstract

We show that LEP II will either discover charginos and neutralinos, or enable a very stringent upper limit to be placed on $\tan \beta$ as a function of the gluino mass. The only assumption we make is the existence of some unified model which breaks down to the minimal supersymmetric standard model below the unification scale. In such a framework we discuss how the discovery of a chargino at LEP II and the measurement of its mass and production cross-section, together with the measurement of the mass of the lightest neutralino, would enable the gluino mass, $\tan \beta$ and μ to be predicted, up to a possible ambiguity in the sign of μ which we discuss.

The LEP e^+e^- collider provides a clean environment for searching for the charginos and neutralinos predicted by the minimal supersymmetric standard model (MSSM) [1]. In the context of a unified model it may be assumed that the three low energy gaugino mass parameters M_i , with $i = 1, 2, 3$ corresponding to the groups $U(1)$, $SU(2)$, and $SU(3)$ respectively, are unified into a universal gaugino mass $M_{1/2}$ at the same scale M_X at which the gauge couplings $\alpha_i = g_i^2/4\pi$ are unified into a single coupling α_X [2]. Then at the electroweak scale (which we take to be m_Z),

$$\frac{M_i}{M_{1/2}} = \frac{\alpha_i(m_Z^2)}{\alpha_X} \quad (1)$$

as a simple consequence of the one-loop renormalisation group equations. For example the gluino mass is given by

$$m_{\tilde{g}} = M_3 = M_{1/2} \frac{\alpha_3(m_Z^2)}{\alpha_X}. \quad (2)$$

Having made this assumption the chargino $\tilde{\chi}_i^\pm$ ($i = 1, 2$) and neutralino $\tilde{\chi}_i^0$ ($i = 1 \dots 4$) masses and mixing angles then only depend on three unknown parameters: the gluino mass $m_{\tilde{g}}$, μ and $\tan \beta$ [3].

Several authors have considered the production of neutralinos and charginos at hadron colliders [4], e^+e^- Colliders at the Z pole [5] and beyond [6], as well as its decay modes [7]. The results of such analyses are usually presented as allowed and excluded regions in the $m_{\tilde{g}} - \mu$ plane for specified values of $\tan \beta$ [8]. Given the already widespread interest in this subject, we should be clear to point out what we have done that has not already been considered. The purpose of the present paper is twofold:

(1) We shall show how existing LEP data may be used to extract a precise bound on $\tan \beta$ as a function of $m_{\tilde{g}}$. In order to do this we shall present our results in the $\tan \beta - \mu$ plane for specified values of $m_{\tilde{g}}$. This enables us to deduce an upper bound on $\tan \beta$ as a function of $m_{\tilde{g}}$. Since the bound is monotonic, the maximum value of $\tan \beta$ is equivalent to specifying the minimum value of $m_{\tilde{g}}$ for a given value of $\tan \beta$, and this information is available from the $\tan \beta = 1, 2, 5, 30$ contours in the $m_{\tilde{g}} - \mu$ plane [8]. However our method makes it possible to extract a precise bound on $\tan \beta$ as a function of $m_{\tilde{g}}$, at LEP.

(2) We shall consider the prospects for chargino discovery at LEP II. Either the chargino will not be discovered, in which case we show that this leads to a very stringent bound on $\tan \beta$ as a function of $m_{\tilde{g}}$. Or the lighter chargino and (by virtue

of its decay) the lightest neutralino will be discovered in which case we show how this would enable the gluino mass, $\tan\beta$ and μ to be predicted from the LEP II measurements of the mass of the chargino, the mass of the lightest neutralino, and the measurement of the chargino production cross-section. We try to present these numerical results in a form which will be useful to experimentalists.

We begin by considering the constraints on the MSSM coming from the negative searches at LEP for new particles with the signatures of charginos and neutralinos. For gluino masses not too heavy, the allowed region of the $\tan\beta$ plane corresponds to negative values of μ ¹ and in practice is determined by the intersection of the regions allowed by the following two constraints:

- The 95% CL upper bound on the contribution of new particles to the Z width is $\Delta\Gamma_Z < 30$ MeV.
- The branching fraction for the decays $Z \rightarrow \tilde{\chi}_i^0 \tilde{\chi}_j^0$ (where i and j are not both 1) satisfies

$$B(Z \rightarrow \tilde{\chi}_i^0 \tilde{\chi}_j^0) < 10^{-5}. \quad (3)$$

The first of these experimental constraints is similar to that used previously [8], and essentially is derived from the measurement of the Z width. This constraint has a similar effect to the constraint that $m_{\tilde{\chi}_1^\pm} > 45$ GeV, (at least for large negative regions of μ) but is always more restrictive for our range of gluino masses. The second constraint above is a factor of 5 more stringent than previously assumed [8]. and is based on the negative searches for typical neutralino signatures such as the preliminary OPAL result [9]

$$B(Z \rightarrow \gamma X_{inv}) < 4.3 \times 10^{-6} \quad (4)$$

for $M_{X_{inv}} < 64$ GeV (95% CL). For our range of gluino mass, this constraint is always more restrictive than the constraint that the invisible width of the Z satisfies $\Delta\Gamma_{Z_{inv}} < 7$ MeV. Constraints such as those mentioned above may be combined by the LEP experiments to produce an excluded region in the $m_{\tilde{\chi}_i^0} - \tan\beta$ plane. For example a preliminary result from L3 gives $m_{\tilde{\chi}_1^0} > 25$ GeV and $m_{\tilde{\chi}_2^0} > 42$ GeV for $\tan\beta > 2$ [9]. We have checked that such excluded regions in the $m_{\tilde{\chi}_i^0} - \tan\beta$ plane do not provide any additional constraints in our analysis, for a sample value of the gluino mass.

¹ We use the same convention as [8] in which the superpotential $W = -\mu H_1 H_2$ where $H_1 H_2 = H_1^0 H_2^0 - H_1^- H_2^+$.

In Fig. 1 we show in detail how the above LEP constraints restrict the parameter space of the MSSM. For a gluino mass of 140 GeV, Fig. 1 shows that much of the $\tan\beta - \mu$ plane is excluded by these constraints. For example all of the parameter space with $\mu > 0$ (mostly not shown) is excluded in this case. In the negative μ region shown in Fig. 1 it is clearly seen that there is a maximum value of $\tan\beta < 5$ given by the intersection of the lines corresponding to the constraints $\Delta\Gamma_Z < 30$ MeV and $B(Z \rightarrow \tilde{\chi}_i^0 \tilde{\chi}_j^0) < 10^{-5}$. The other constraints mentioned above are shown for completeness in Fig. 1 but do not provide additional restrictions on the allowed region of the $\tan\beta - \mu$ plane. However if LEPII fails to discover the lighter chargino and sets a limit of $m_{\tilde{\chi}_1^\pm} > 80$ GeV, then the effect dramatically reduces the allowed region in this plane to the very small region indicated near $\tan\beta \approx 1$ and $\mu \approx -80$ GeV.

From analysing plots of the kind shown in Fig. 1 for various gluino masses we are able to obtain a rather precise upper bound on $\tan\beta$ as a function of gluino mass from existing LEP data, and a corresponding but much more restrictive bound on $\tan\beta$ from the assumption that LEPII will not discover the chargino, and will set a limit of $m_{\tilde{\chi}_1^\pm} > 80$ GeV. Both these bounds are shown in Fig. 2. The model independent bound on the gluino mass from CDF is $m_{\tilde{g}} > 100$ GeV (90 % c.l.) [10].² These plots show that, should an intermediate mass gluino be discovered at the Tevatron, then a precise and useful bound may be placed upon $\tan\beta$ by LEPI or LEPII data, on the assumption that no charginos or neutralinos are discovered at LEPII.

A light gluino is not excluded by experiments [12]. The allowed light gluino window is $2.6 < m_{\tilde{g}} \lesssim 6$ GeV and $m_{\tilde{g}} < 0.6$ GeV, although the exact boundary of this window is controversial [13]. With the assumptions presented in this paper, i. e. , unification of gaugino masses, there is an allowed region in the $\tan\beta - \mu$ plane [14, 15]. Nevertheless, in supergravity models with a radiatively broken electroweak symmetry group and universality of scalar and gaugino masses at the unification scale the light gluino window has been closed [15].

Now let us consider the possibility that LEPII will discover the lighter chargino with a mass in the range $m_{\tilde{\chi}_1^\pm} = 50 - 90$ GeV. A typical signature of chargino pair production would be a charged lepton pair l^+l^- plus missing energy, arising from the decay $\tilde{\chi}_1^\pm \rightarrow \tilde{\chi}_1^0 W^{\pm*}$, $W^{\pm*} \rightarrow l^\pm \nu$. Such a clean signature should enable the chargino to be discovered right up to the kinematic limit of the collider, and by scanning in energy the chargino mass should be easily extracted. Clearly if LEPII

²This bound allows the squarks to be heavier than the gluino, and allows cascade decays [11].

discovers the lighter chargino then it will simultaneously also discover the lightest neutralino into which the chargino decays thereby discovering two new particles for the price of one! By various kinematic means, such as measuring the maximum charged lepton momenta, it should be possible to measure the lightest neutralino mass from such events. Given accurate measurements of $m_{\tilde{\chi}_1^\pm}$, $m_{\tilde{\chi}_1^0}$ and the total cross-section $\sigma(e^+e^- \rightarrow \tilde{\chi}_1^+ \tilde{\chi}_1^-)$ it will be possible for LEP II to pin down all the parameters of the chargino/neutralino sector, namely $m_{\tilde{g}}$, $\tan\beta$ and μ , from which all the information about the entire chargino/neutralino spectrum may be determined, assuming unification.

In Figs. 3-7 we show gluino mass contours in the $\sigma(e^+e^- \rightarrow \tilde{\chi}_1^+ \tilde{\chi}_1^-) - m_{\tilde{\chi}_1^0}$ plane for chargino masses of $m_{\tilde{\chi}_1^\pm} = 50 - 90$ GeV.³ In each of the figures, we have fixed the chargino mass, and plotted the cross-section as a function of the lightest neutralino, for an allowed range of gluino masses. These plots clearly show that the LEP II measurements of the lightest chargino and neutralino masses (and to a lesser extent the cross-section) enable the gluino mass to be predicted from the theory. Furthermore the values of $\tan\beta$ and μ given at the end-points of the gluino mass contours will vary along the contour, thus enabling these parameters to be pinned down by an accurate measurement of the cross-section. The precise accuracy required is clear from these figures. The finite length of the contours in Figs. 3-7 is due to the Z-pole constraints discussed earlier, and so for example $\tan\beta$ will vary along each of the contours up to its maximum permitted value. In some of the contours it will be noticed that there is a small gap. This gap corresponds to two different allowed regions with different signs of μ . These broken contours occur for heavier values of gluino mass and generally have a hairpin shape. By contrast the contours for lighter gluino masses are approximately vertical straight lines, and only have an allowed region for negative μ . The broken-hairpin contours tend to intersect other contours leading to ambiguities in the determination of μ , $\tan\beta$ and $m_{\tilde{g}}$ which may be resolved by a direct measurement of the gluino mass, for example.

Corresponding to Figs. 3-7, Tables 1-5 show the ranges of $\tan\beta$ and μ for each of the contours. In these Tables we have also included the corresponding ranges of the cross-section and lightest neutralino mass which will enable the entries in Tables 1-5 to be identified with the contours in Figs. 3-7. The region where the contours

³We have neglected the diagrams involving virtual sneutrinos, and assume that $\sigma(e^+e^- \rightarrow \tilde{\chi}_1^+ \tilde{\chi}_1^-) \approx \sigma(e^+e^- \rightarrow Z^*, \gamma^* \rightarrow \tilde{\chi}_1^+ \tilde{\chi}_1^-)$. This should be a good approximation provided the sneutrino mass exceeds 500 GeV. Also we have assumed that the SUSY breaking scale is equal to m_Z which is consistent for gluino masses of order 100 GeV.

are approximately vertical is particularly interesting. A measurement of the lightest chargino and neutralino masses in that region predicts the gluino mass independently of the value of the total cross section. This prediction is therefore independent of the sneutrino mass, which we have neglected. This can be understood in the following way: if the sneutrino is lighter than about 500 GeV, its contribution to the total cross section starts to become non-negligible and the value of $\sigma(e^+e^- \rightarrow \tilde{\chi}_1^+ \tilde{\chi}_1^-)$ will change with respect to our approximation, but the chargino/neutralino spectrum will be unaffected. This implies that, although the vertical contours move up and down the vertical axis when the sneutrino mass is changed, the prediction of the gluino mass remains unchanged. Another property of this region is that the value of the parameter $\tan\beta$ is confined to a narrow interval close to the unity. This type of upper bound on $\tan\beta$ is precisely what we have in Fig. 2.

We hope that the combination of Figs. 3-7 and Tables 1-5 will prove useful in drawing the first conclusions about the parameters μ , $\tan\beta$ and $m_{\tilde{g}}$ from the experimental measurements of $\sigma(e^+e^- \rightarrow \tilde{\chi}_1^+ \tilde{\chi}_1^-)$, $m_{\tilde{\chi}_1^0}$ and $m_{\tilde{\chi}_1^\pm}$. With knowledge of μ , $\tan\beta$ and $m_{\tilde{g}}$ one may predict the entire spectrum of chargino and neutralino masses and mixing angles using standard formulae, and then search for the remaining particles in this sector. The particle physics and cosmological implications can hardly be overstated, and so it is with some excitement that we await the first results from LEP II.

Table 1. The numerical values of $\tan\beta$, μ (GeV), $\sigma(e^+e^- \rightarrow \tilde{\chi}_1^+ \tilde{\chi}_1^-)$ (pb), $m_{\tilde{\chi}_1^0}$ (GeV) at the end-points of the gluino contours in Fig. 3 corresponding to $m_{\tilde{\chi}_1^\pm}=50$ GeV.

$m_{\tilde{g}}$	$\tan\beta$	μ	σ	$m_{\tilde{\chi}_1^0}$
100	$1.00 \rightarrow 1.62$	$-270 \rightarrow -227$	$7.48 \rightarrow 7.35$	17.9
110	$1.00 \rightarrow 1.75$	$-326 \rightarrow -263$	$7.58 \rightarrow 7.45$	$19.4 \rightarrow 19.5$
120	$1.00 \rightarrow 1.95$	$-406 \rightarrow -303$	$7.67 \rightarrow 7.53$	$20.9 \rightarrow 21.0$
130	$1.00 \rightarrow 2.30$	$-528 \rightarrow -348$	$7.74 \rightarrow 7.60$	22.3
140	$1.00 \rightarrow 2.87$	$-741 \rightarrow -400$	$7.80 \rightarrow 7.65$	$23.5 \rightarrow 23.6$
160	$5.03 \rightarrow 7.40$	$-991 \rightarrow -503$	$7.82 \rightarrow 7.71$	$25.6 \rightarrow 25.7$
180	$3.42 \rightarrow 9.91$	$995 \rightarrow 506$	$7.82 \rightarrow 7.70$	$26.8 \rightarrow 27.0$
200	$1.00 \rightarrow 3.07$	$707 \rightarrow 462$	$7.77 \rightarrow 7.65$	$27.3 \rightarrow 27.5$
220	$1.00 \rightarrow 2.04$	$458 \rightarrow 382$	$7.62 \rightarrow 7.53$	$27.2 \rightarrow 27.4$
250	$1.00 \rightarrow 1.69$	$310 \rightarrow 282$	$7.31 \rightarrow 7.21$	$26.5 \rightarrow 26.8$
300	$1.00 \rightarrow 22.9$	$212 \rightarrow 100$	$6.64 \rightarrow 5.33$	$25.2 \rightarrow 31.0$
400	$1.00 \rightarrow 4.57$	$142 \rightarrow 100$	$5.40 \rightarrow 4.82$	$24.7 \rightarrow 29.6$
600	$1.00 \rightarrow 4.37$	$99.7 \rightarrow 77.0$	$4.14 \rightarrow 3.93$	$28.3 \rightarrow 32.2$
800	$1.00 \rightarrow 100$	$84.0 \rightarrow 56.1$	$3.71 \rightarrow 3.57$	$32.5 \rightarrow 35.3 \rightarrow 35.2$
”	$50.1 \rightarrow 2.00$	$-54.4 \rightarrow -33.2$	$3.56 \rightarrow 3.48$	$35.1 \rightarrow 30.3$
1000	$1.00 \rightarrow 100$	$75.8 \rightarrow 54.0$	$3.52 \rightarrow 3.45$	$35.8 \rightarrow 37.3 \rightarrow 37.1$
”	$100 \rightarrow 1.74$	$-53.1 \rightarrow -34.5$	$3.45 \rightarrow 3.40$	$37.0 \rightarrow 32.8$

Table 2. The numerical values of $\tan\beta$, μ (GeV), $\sigma(e^+e^- \rightarrow \tilde{\chi}_1^+ \tilde{\chi}_1^-)$ (pb), $m_{\tilde{\chi}_1^0}$ (GeV) at the end-points of the gluino contours in Fig. 4 corresponding to $m_{\tilde{\chi}_1^\pm} = 60$ GeV.

$m_{\tilde{g}}$	$\tan\beta$	μ	σ	$m_{\tilde{\chi}_1^0}$
100	1.00 \rightarrow 1.46	-154 \rightarrow -130	6.86 \rightarrow 6.67	18.2
110	1.00 \rightarrow 1.57	-177 \rightarrow -143	6.99 \rightarrow 6.75	19.9
120	1.00 \rightarrow 1.69	-207 \rightarrow -158	7.10 \rightarrow 6.83	21.5 \rightarrow 21.6
130	1.00 \rightarrow 1.87	-245 \rightarrow -171	7.21 \rightarrow 6.89	23.1 \rightarrow 23.2
140	1.00 \rightarrow 2.08	-295 \rightarrow -185	7.31 \rightarrow 6.95	24.6 \rightarrow 24.7
160	1.00 \rightarrow 2.85	-469 \rightarrow -193	7.48 \rightarrow 6.94	27.3 \rightarrow 27.6
180	1.00 \rightarrow 4.07	-981 \rightarrow -276	7.58 \rightarrow 7.20	29.6 \rightarrow 29.9
200	21.9 \rightarrow 5.25	-985 \rightarrow -145	7.58 \rightarrow 6.40	31.3 \rightarrow 32.8
220	1.91 \rightarrow 100	987 \rightarrow 271	7.58 \rightarrow 7.09	32.4 \rightarrow 33.2
"	100 \rightarrow 5.50	-248 \rightarrow -115	7.01 \rightarrow 5.90	33.3 \rightarrow 35.1
250	1.00 \rightarrow 100	496 \rightarrow 169	7.41 \rightarrow 6.38	32.9 \rightarrow 35.5
"	100 \rightarrow 4.79	-159 \rightarrow -84.7	6.29 \rightarrow 5.21	35.7 \rightarrow 37.6
300	1.00 \rightarrow 100	277 \rightarrow 121	6.88 \rightarrow 5.51	32.5 \rightarrow 37.7
"	100 \rightarrow 4.37	-116 \rightarrow -67.8	5.43 \rightarrow 4.61	37.9 \rightarrow 39.0 \rightarrow 38.4
400	1.00 \rightarrow 100	168 \rightarrow 90.5	5.59 \rightarrow 4.50	32.2 \rightarrow 39.3
"	100 \rightarrow 1.00	-87.6 \rightarrow -24.2	4.46 \rightarrow 3.63	39.5 \rightarrow 39.7 \rightarrow 24.2
600	1.00 \rightarrow 100	114 \rightarrow 73.1	4.13 \rightarrow 3.73	36.2 \rightarrow 41.8
"	100 \rightarrow 1.00	-71.4 \rightarrow -33.1	3.72 \rightarrow 3.44	41.8 \rightarrow 33.1
800	1.00 \rightarrow 100	95.9 \rightarrow 67.4	3.64 \rightarrow 3.47	41.0 \rightarrow 44.3
"	100 \rightarrow 1.00	-66.2 \rightarrow -38.5	3.46 \rightarrow 3.34	44.3 \rightarrow 38.5
1000	1.00 \rightarrow 100	86.9 \rightarrow 64.8	3.44 \rightarrow 3.35	44.7 \rightarrow 46.5
"	100 \rightarrow 1.00	-63.9 \rightarrow -42.1	3.35 \rightarrow 3.28	46.4 \rightarrow 42.1

Table 3. The numerical values of $\tan\beta$, μ (GeV), $\sigma(e^+e^- \rightarrow \tilde{\chi}_1^+ \tilde{\chi}_1^-)$ (pb), $m_{\tilde{\chi}_1^0}$ (GeV) at the end-points of the gluino contours in Fig. 5 corresponding to $m_{\tilde{\chi}_1^\pm} = 70$ GeV.

$m_{\tilde{g}}$	$\tan\beta$	μ	σ	$m_{\tilde{\chi}_1^0}$
100	$1.00 \rightarrow 1.27$	$-90.5 \rightarrow -80.3$	$6.05 \rightarrow 5.89$	18.4
110	$1.00 \rightarrow 1.38$	$-103 \rightarrow -84.0$	$6.17 \rightarrow 5.89$	20.2
120	$1.00 \rightarrow 1.49$	$-119 \rightarrow -86.0$	$6.30 \rightarrow 5.87$	21.9
130	$1.00 \rightarrow 1.60$	$-137 \rightarrow -89.4$	$6.42 \rightarrow 5.86$	$23.5 \rightarrow 23.7$
140	$1.00 \rightarrow 1.73$	$-159 \rightarrow -89.1$	$6.54 \rightarrow 5.79$	$25.1 \rightarrow 25.4$
160	$1.00 \rightarrow 1.98$	$-220 \rightarrow -103$	$6.76 \rightarrow 5.89$	$28.2 \rightarrow 28.6$
180	$1.00 \rightarrow 2.31 \rightarrow 2.20$	$-328 \rightarrow -84.3$	$6.95 \rightarrow 5.42$	$31.0 \rightarrow 31.9$
200	$1.00 \rightarrow 2.95 \rightarrow 2.40$	$-561 \rightarrow -81.4$	$7.08 \rightarrow 5.22$	$33.4 \rightarrow 35.0$
220	$2.34 \rightarrow 4.57 \rightarrow 2.40$	$-999 \rightarrow -70.2$	$7.14 \rightarrow 4.83$	$35.4 \rightarrow 37.9$
250	$2.63 \rightarrow 100$	$1000 \rightarrow 325$	$7.14 \rightarrow 6.81$	$37.5 \rightarrow 38.1$
”	$100 \rightarrow 2.40$	$-297 \rightarrow -62.7$	$6.75 \rightarrow 4.45$	$38.3 \rightarrow 41.3 \rightarrow 41.2$
300	$1.00 \rightarrow 100$	$397 \rightarrow 162$	$6.84 \rightarrow 5.77$	$38.7 \rightarrow 42.1$
”	$100 \rightarrow 1.66$	$-154 \rightarrow -40.2$	$5.69 \rightarrow 3.72$	$42.4 \rightarrow 44.9 \rightarrow 36.5$
400	$1.00 \rightarrow 100$	$200 \rightarrow 109$	$5.65 \rightarrow 4.49$	$39.1 \rightarrow 46.2$
”	$100 \rightarrow 1.00$	$-106 \rightarrow -36.1$	$4.44 \rightarrow 3.38$	$46.4 \rightarrow 47.6 \rightarrow 36.1$
600	$1.00 \rightarrow 100$	$129 \rightarrow 85.8$	$4.03 \rightarrow 3.57$	$43.7 \rightarrow 50.2$
”	$100 \rightarrow 1.00$	$-84.1 \rightarrow -44.2$	$3.55 \rightarrow 3.22$	$50.3 \rightarrow 50.6 \rightarrow 44.2$
800	$1.00 \rightarrow 100$	$108 \rightarrow 78.7$	$3.47 \rightarrow 3.28$	$49.3 \rightarrow 53.4$
”	$100 \rightarrow 1.00$	$-77.5 \rightarrow -49.2$	$3.28 \rightarrow 3.13$	$53.4 \rightarrow 49.2$
1000	$1.00 \rightarrow 100$	$98.1 \rightarrow 75.6$	$3.26 \rightarrow 3.17$	$53.5 \rightarrow 55.9$
”	$100 \rightarrow 1.00$	$-74.7 \rightarrow -52.6$	$3.16 \rightarrow 3.09$	$55.9 \rightarrow 52.6$

Table 4. The numerical values of $\tan\beta$, μ (GeV), $\sigma(e^+e^- \rightarrow \tilde{\chi}_1^+ \tilde{\chi}_1^-)$ (pb), $m_{\tilde{\chi}_1^0}$ (GeV) at the end-points of the gluino contours in Fig. 6 corresponding to $m_{\tilde{\chi}_1^\pm}=80$ GeV.

$m_{\tilde{g}}$	$\tan\beta$	μ	σ	$m_{\tilde{\chi}_1^0}$
123	1.00 \rightarrow 1.06	-68.9 \rightarrow -68.1	5.27 \rightarrow 5.25	22.6
130	1.00 \rightarrow 1.19	-76.5 \rightarrow -68.1	5.35 \rightarrow 5.17	23.8 \rightarrow 23.9
140	1.00 \rightarrow 1.29	-88.7 \rightarrow -69.3	5.46 \rightarrow 5.09	25.5 \rightarrow 25.6
160	1.00 \rightarrow 1.45	-120 \rightarrow -76.1	5.68 \rightarrow 5.03	28.8 \rightarrow 29.0
180	1.00 \rightarrow 1.58	-166 \rightarrow -66.4	5.89 \rightarrow 4.58	31.9 \rightarrow 32.5
200	1.00 \rightarrow 1.88 \rightarrow 1.66	-239 \rightarrow -63.8	6.08 \rightarrow 4.30	34.7 \rightarrow 35.9
220	1.00 \rightarrow 2.19 \rightarrow 1.74	-373 \rightarrow -63.6	6.23 \rightarrow 4.12	37.3 \rightarrow 39.0
250	1.65 \rightarrow 3.84 \rightarrow 1.34	-996 \rightarrow -44.1	6.36 \rightarrow 3.34	40.4 \rightarrow 43.5 \rightarrow 41.8
300	1.00 \rightarrow 100	743 \rightarrow 245	6.32 \rightarrow 5.78	43.5 \rightarrow 45.0
"	100 \rightarrow 1.00	-231 \rightarrow -42.1	5.72 \rightarrow 3.09	45.1 \rightarrow 49.1 \rightarrow 42.1
400	1.00 \rightarrow 100	243 \rightarrow 132	5.41 \rightarrow 4.32	45.4 \rightarrow 51.7
"	100 \rightarrow 1.00	-128 \rightarrow -47.8	4.26 \rightarrow 2.98	52.0 \rightarrow 54.8 \rightarrow 47.8
600	1.00 \rightarrow 100	145 \rightarrow 98.8	3.74 \rightarrow 3.24	50.8 \rightarrow 58.2
"	100 \rightarrow 1.00	-97.1 \rightarrow -55.2	3.23 \rightarrow 2.85	58.4 \rightarrow 59.3 \rightarrow 55.2
800	1.00 \rightarrow 100	120 \rightarrow 90.2	3.15 \rightarrow 2.95	57.2 \rightarrow 62.3
"	100 \rightarrow 1.00	-89.0 \rightarrow -59.8	2.94 \rightarrow 2.78	62.3 \rightarrow 62.6 \rightarrow 59.8
1000	1.00 \rightarrow 100	109 \rightarrow 86.4	2.92 \rightarrow 2.83	62.2 \rightarrow 65.2
"	100 \rightarrow 1.00	-85.5 \rightarrow -63.0	2.82 \rightarrow 2.75	65.2 \rightarrow 63.0

Table 5. The numerical values of $\tan\beta$, μ (GeV), $\sigma(e^+e^- \rightarrow \tilde{\chi}_1^+ \tilde{\chi}_1^-)$ (pb), $m_{\tilde{\chi}_1^0}$ (GeV) at the end-points of the gluino contours in Fig. 6 corresponding to $m_{\tilde{\chi}_1^\pm}=90$ GeV.

$m_{\tilde{g}}$	$\tan\beta$	μ	σ	$m_{\tilde{\chi}_1^0}$
160	1.00 \rightarrow 1.05	-62.6 \rightarrow -61.0	4.11 \rightarrow 4.05	29.3
180	1.00 \rightarrow 1.21	-87.9 \rightarrow -70.8	4.28 \rightarrow 3.93	32.5 \rightarrow 32.7
200	1.00 \rightarrow 1.36 \rightarrow 1.24	-123 \rightarrow -56.5	4.45 \rightarrow 3.05	35.6 \rightarrow 36.3
220	1.00 \rightarrow 1.52 \rightarrow 1.23	-176 \rightarrow -54.8	4.61 \rightarrow 2.75	38.5 \rightarrow 39.7
250	1.00 \rightarrow 2.00 \rightarrow 1.00	-332 \rightarrow -50.9	4.80 \rightarrow 2.40	42.3 \rightarrow 45.0
300	14.5 \rightarrow 1.00	-962 \rightarrow -54.2	4.92 \rightarrow 2.36	47.0 \rightarrow 53.4
400	1.00 \rightarrow 100	307 \rightarrow 160	4.47 \rightarrow 3.67	50.9 \rightarrow 55.7
"	100 \rightarrow 1.00	-155 \rightarrow -59.3	3.62 \rightarrow 2.28	56.0 \rightarrow 61.3 \rightarrow 59.3
600	1.00 \rightarrow 100	162 \rightarrow 112	3.03 \rightarrow 2.57	57.4 \rightarrow 65.5
"	100 \rightarrow 1.00	-111 \rightarrow -66.1	2.56 \rightarrow 2.19	65.8 \rightarrow 68.1 \rightarrow 66.1
800	1.00 \rightarrow 100	133 \rightarrow 102	2.48 \rightarrow 2.30	64.9 \rightarrow 70.9
"	100 \rightarrow 1.00	-100 \rightarrow -70.5	2.29 \rightarrow 2.15	71.0 \rightarrow 71.9 \rightarrow 70.5
1000	1.00 \rightarrow 100	121 \rightarrow 97.3	2.28 \rightarrow 2.19	70.6 \rightarrow 74.4
"	100 \rightarrow 1.00	-96.4 \rightarrow -73.5	2.19 \rightarrow 2.12	74.4 \rightarrow 74.7 \rightarrow 73.5

References

- [1] H.P. Nilles, *Phys. Rep.* **110**, 1 (1984); H.E. Haber and G.L. Kane, *Phys. Rep.* **117**, 75 (1985); R. Barbieri, *Riv. Nuovo Cimento* **11**, 1 (1988).
- [2] M.B. Einhorn and D.T.R. Jones, *Nucl. Phys.* **B196**, 475 (1982); W.. Marciano and G. Senjanovic, *Phys. Rev. D* **25**, 3092 (1982); U. Amaldi et al. , *Phys. Rev. D* **36**, 1385 (1987); U. Amaldi et al. , *Phys. Lett. B* **260**, 447 (1991); U. Amaldi et al. , *Phys. Lett. B* **281**, 374 (1992).
- [3] J.F. Gunion and H.E. Haber, *Nucl. Phys.* **B272**, 1 (1986).
- [4] H. Baer, V. Barger, R.J.N. Phillips, and X. Tata, *Phys. Lett. B* **220**, 303 (1989); R. Barbieri, F. Caravaglios, M. Frigeni, and M.L. Mangano, *Nucl. Phys.* **B367**, 28 (1991); H. Baer and X. Tata, *Phys. Rev.* **47**, 2739 (1993); H. Baer, C. Kao, and X. Tata, *Phys. Rev. D* **48**, 5175 (1993); H. Baer, C. Chen, F. Paige, and X. Tata, *Phys. Rev. D* **50**, 4508 (1994).
- [5] H. Komatsu and J. Kubo, *Phys. Lett.* **162B**, 379 (1985); R. Barbieri, G. Gamberini, G.F. Giudice, and G. Ridolfi, *Phys. Lett.* **195B**, 500 (1987); M.S. Carena and C.E.M. Wagner, *Phys. Lett.* **195B**, 599 (1987); H. Konig, U. Ellwanger, and M.G. Schmidt, *Z. Phys.* **C36**, 715 (1987); A. Bartl, W. Majerotto, and N. Oshimo, *Phys. Lett. B* **216**, 233 (1989); A. Bartl, S. Stippel, W. Majerotto, and N. Oshimo, *Phys. Lett. B* **233**, 241 (1989); A. Bartl, W. Majerotto, N. Oshimo, and S. Stippel, *Z. Phys.* **C47**, 235 (1990); K. Hidaka and P. Ratcliffe, *Phys. Lett. B* **252**, 476 (1990).
- [6] A. Bartl, H. Fraas, and W. Majerotto, *Z. Phys.* **C30**, 441 (1986); A. Bartl, H. Fraas, and W. Majerotto, *Nucl. Phys.* **B278**, 1 (1986); A. Bartl, H. Fraas, W. Majerotto, and B. Mosslacher, *Z. Phys.* **C55**, 257 (1992); M.H. Nous, M. El-Kishen, and T.A. El-Azem, *Mod. Phys. Lett.* **A7**, 1535 (1992); J. Feng and M. Strassler, Report No. SLAC-PUB-6497, August 1994.
- [7] J.F. Gunion et al. , *Int. J. Mod. Phys.* **A2**, 1147 (1987); J.F. Gunion and H.E. Haber, *Phys. Rev. D* **37**, 2515 (1988); H.E. Haber and D. Wyler, *Nucl. Phys.* **B323**, 267 (1989); Y. Kizukuri and N. Oshimo, *Phys. Lett. B* **220**, 293 (1989); J.H. Reid, E.J.O. Gavin, and M.A. Samuel, *Phys. Rev. D* **49**, 2382 (1994).
- [8] H. Baer and X. Tata, Report No. FSU-HEP-921222, Dec. 1992.

- [9] M. Pohl, “Search For New Particles and New Interactions”, ICHEP 94, Glasgow, July 25, 1994.
- [10] Review of Particle Properties, *Phys. Rev.* **D50** (1994) p.1803.
- [11] H. Baer, X. Tata, and J. Woodside, *Phys. Rev. D* **41**, 906 (1990); and *Phys. Rev. D* **44**, 207 (1991).
- [12] P.M. Tuts et al. , *Phys. Lett. B* **186**, 233 (1987); UA1 Collaboration, C. Albajar et al. , *Phys. Lett. B* **198**, 261 (1987).
- [13] H.E. Haber, Report No. SCIPP 93/21, 1993; R.M. Barnett, H.E. Haber, and G.L. Kane, *Nucl. Phys.* **B267**, 625 (1986); M.B. Cakir and G.R. Farrar, *Phys. Rev. D* **50**, 3268 (1994).
- [14] F. de Campos and J.W.F. Valle, Report No. FTUV/93-9, Feb. 1993; J.L. Lopez, D.V. Nanopoulos, and X. Wang, *Phys. Lett. B* **313**, 241 (1993); M. Carena, L. Clavelli, D. Matalliotakis, H.P. Nilles, and C.E.M. Wagner, *Phys. Lett. B* **317**, 346 (1993);
- [15] M.A. Díaz, *Phys. Rev. Lett.* **73**, 2409 (1994).

Figure Captions:

Fig. 1. Allowed region in the $\tan\beta - \mu$ plane for $m_{\tilde{g}} = 140$ GeV. The different regions below each curve correspond to the following constraints: $m_{\tilde{\chi}_1^\pm} \geq 45$ GeV (large solid curve), $\Delta\Gamma_Z \leq 30$ MeV (dashes), $\Delta\Gamma_Z^{inv} \leq 7$ MeV (dotdash), $B(Z \rightarrow \tilde{\chi}_i^0 \tilde{\chi}_j^0) \leq 1 \times 10^{-5}$ (dots), and, in the case a new lower bound on the chargino mass is found, $m_{\tilde{\chi}_1^\pm} \geq 80$ GeV (small solid curve).

Fig. 2. Gluino mass dependent upper bound on $\tan\beta$. The curve on the left corresponds to the LEP data, and the curve on the right corresponds to a hypothetical new lower bound on the chargino mass ($m_{\tilde{\chi}_1^\pm} > 80$ GeV) at LEP II. In each case, the allowed region lies below and at the right of the curve. The experimental lower bound on the gluino mass is 100 GeV, with the exception of the light gluino window (see the text).

Fig. 3. For a chargino mass given by $m_{\tilde{\chi}_1^\pm} = 50$ GeV, we plot contours of equal gluino mass $m_{\tilde{g}} = 100, 110, 120, 130, 140, 160, 180, 200, 220, 250, 300, 400, 600, 800, 1000$ GeV, in the plane $\sigma(e^+e^- \rightarrow Z^*, \gamma^* \rightarrow \chi_1^+ \chi_1^-) - m_{\chi_1^0}$.

Fig. 4. Same as Fig. 3 with $m_{\tilde{\chi}_1^\pm} = 60$ GeV.

Fig. 5. Same as Fig. 3 with $m_{\tilde{\chi}_1^\pm} = 70$ GeV.

Fig. 6. Same as Fig. 3 with $m_{\tilde{\chi}_1^\pm} = 80$ GeV and for gluino masses given by $m_{\tilde{g}} = 123, 130, 140, 160, 180, 200, 220, 250, 300, 400, 600, 800, 1000$ GeV.

Fig. 7. Same as Fig. 3 with $m_{\tilde{\chi}_1^\pm} = 90$ GeV and for gluino masses given by $m_{\tilde{g}} = 160, 180, 200, 220, 250, 300, 400, 600, 800, 1000$ GeV.

This figure "fig1-1.png" is available in "png" format from:

<http://arxiv.org/ps/hep-ph/9501228v1>

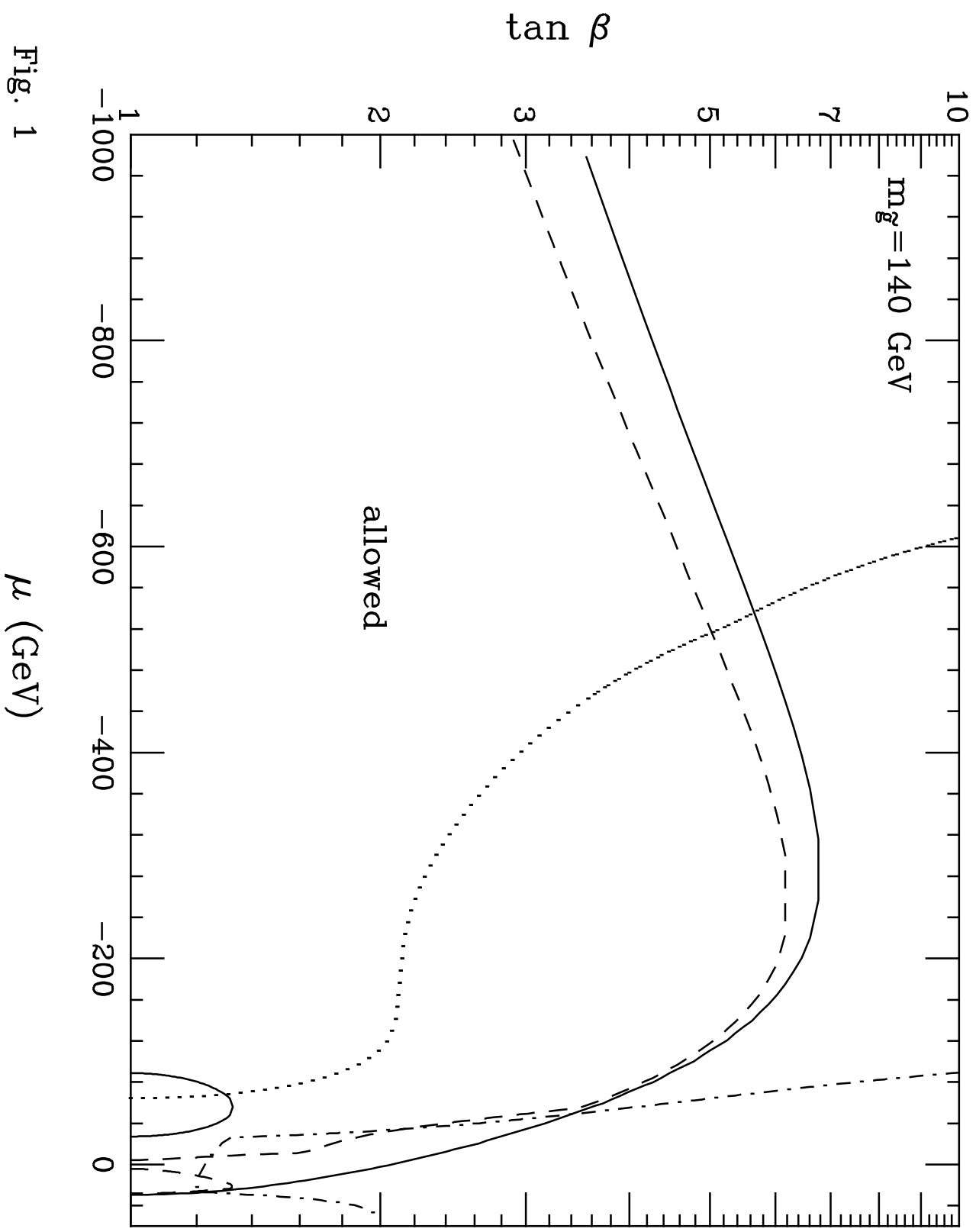


Fig. 1

This figure "fig1-2.png" is available in "png" format from:

<http://arxiv.org/ps/hep-ph/9501228v1>

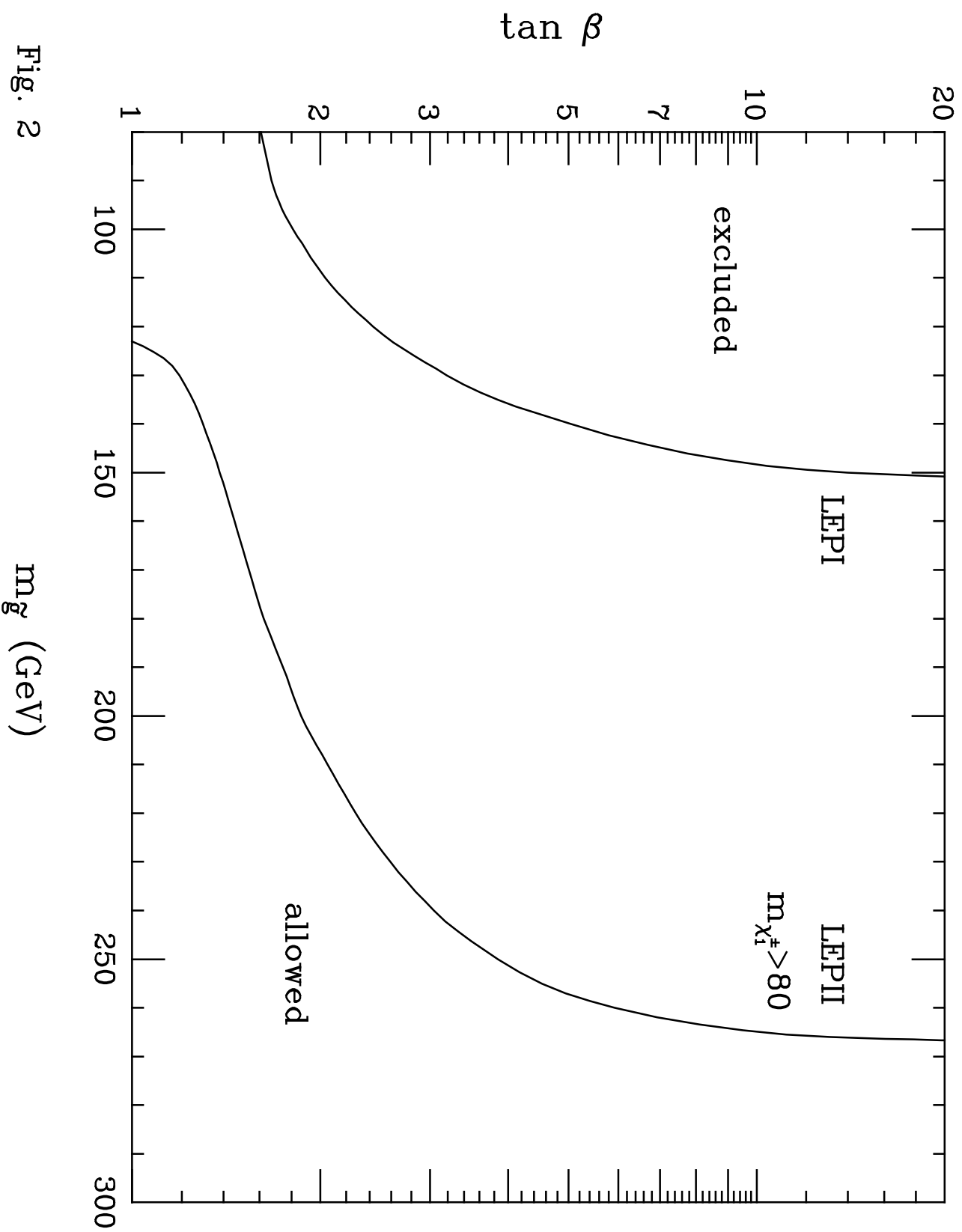


Fig. 2

This figure "fig1-3.png" is available in "png" format from:

<http://arxiv.org/ps/hep-ph/9501228v1>

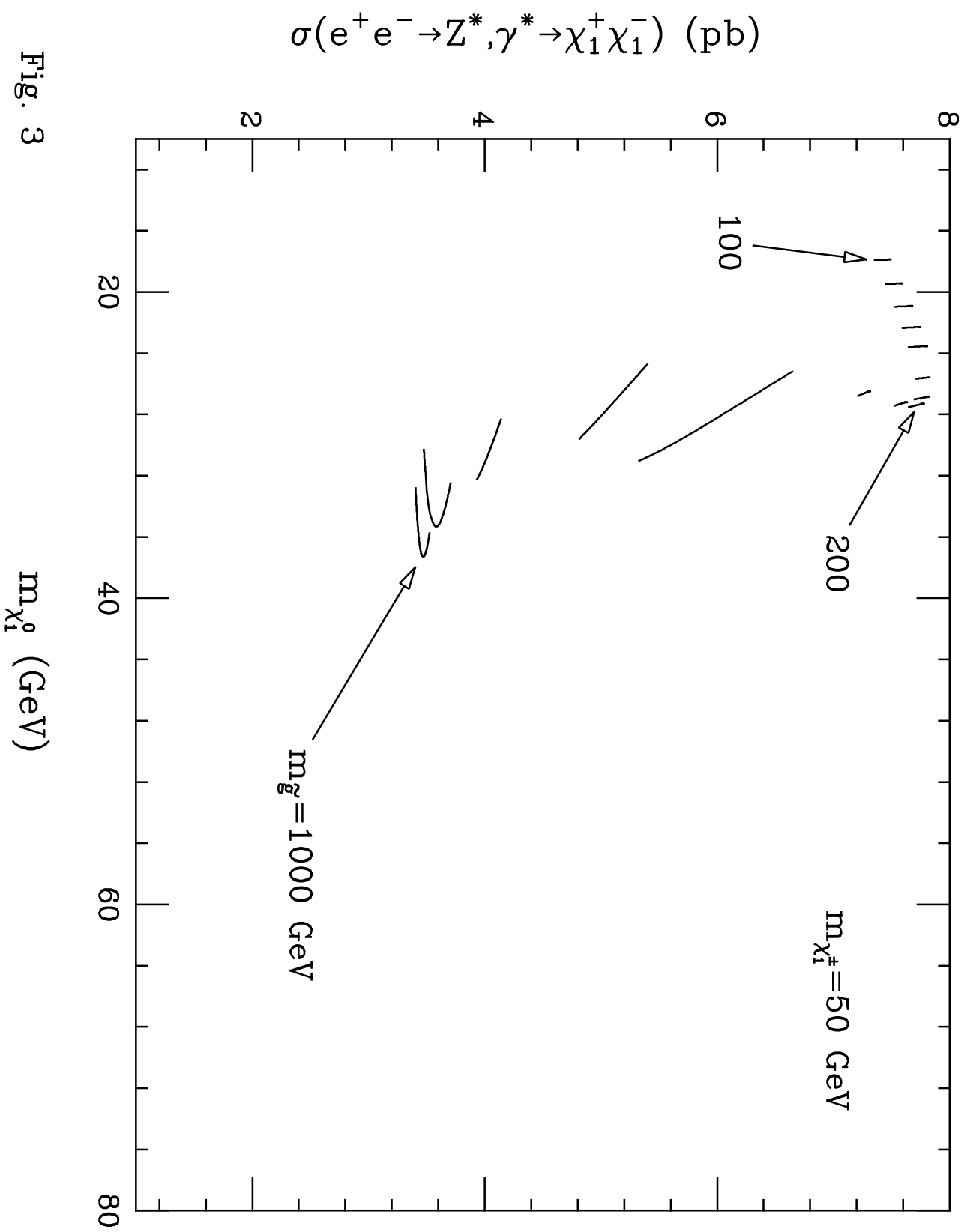


Fig. 3

This figure "fig1-4.png" is available in "png" format from:

<http://arxiv.org/ps/hep-ph/9501228v1>

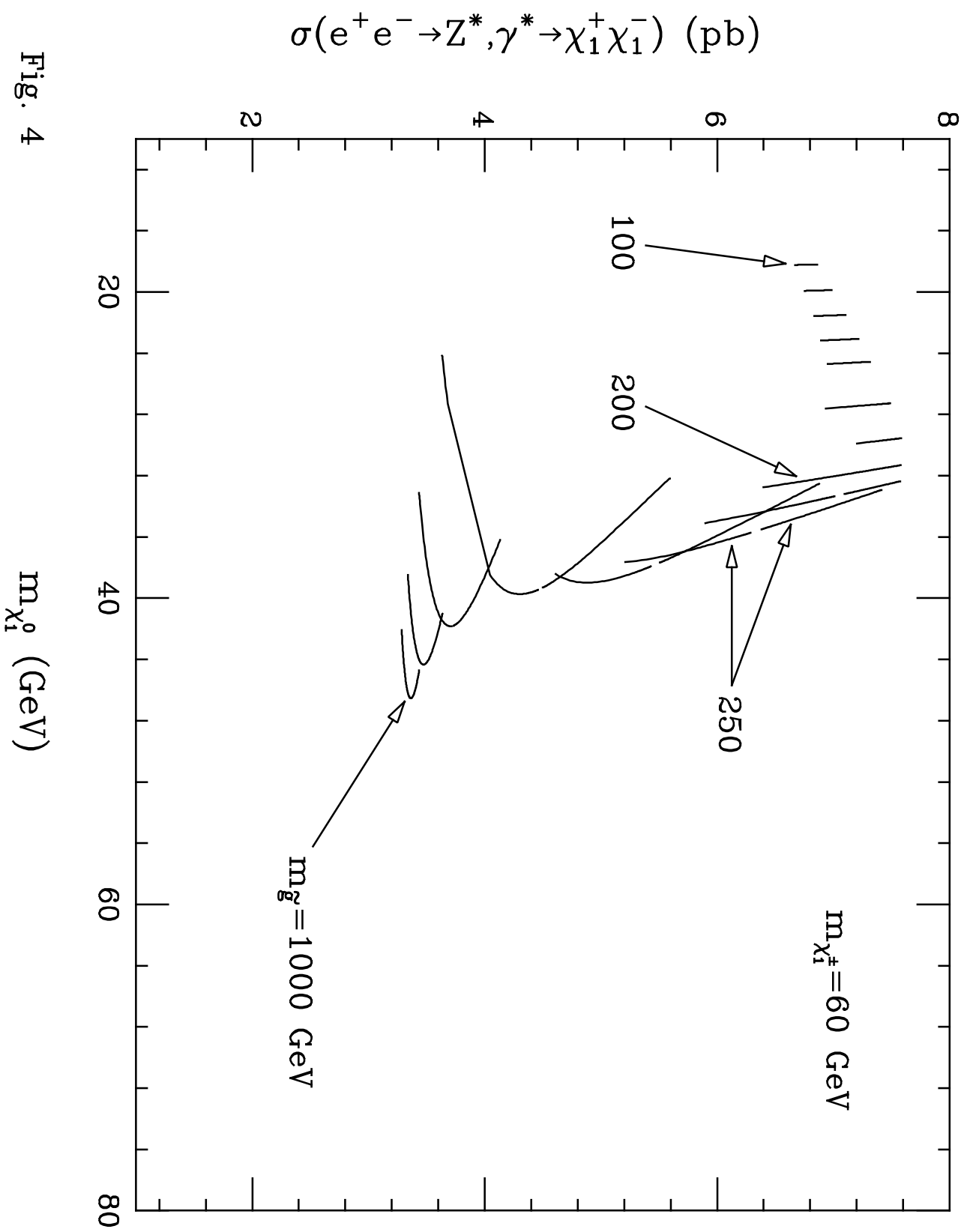


Fig. 4

This figure "fig1-5.png" is available in "png" format from:

<http://arxiv.org/ps/hep-ph/9501228v1>

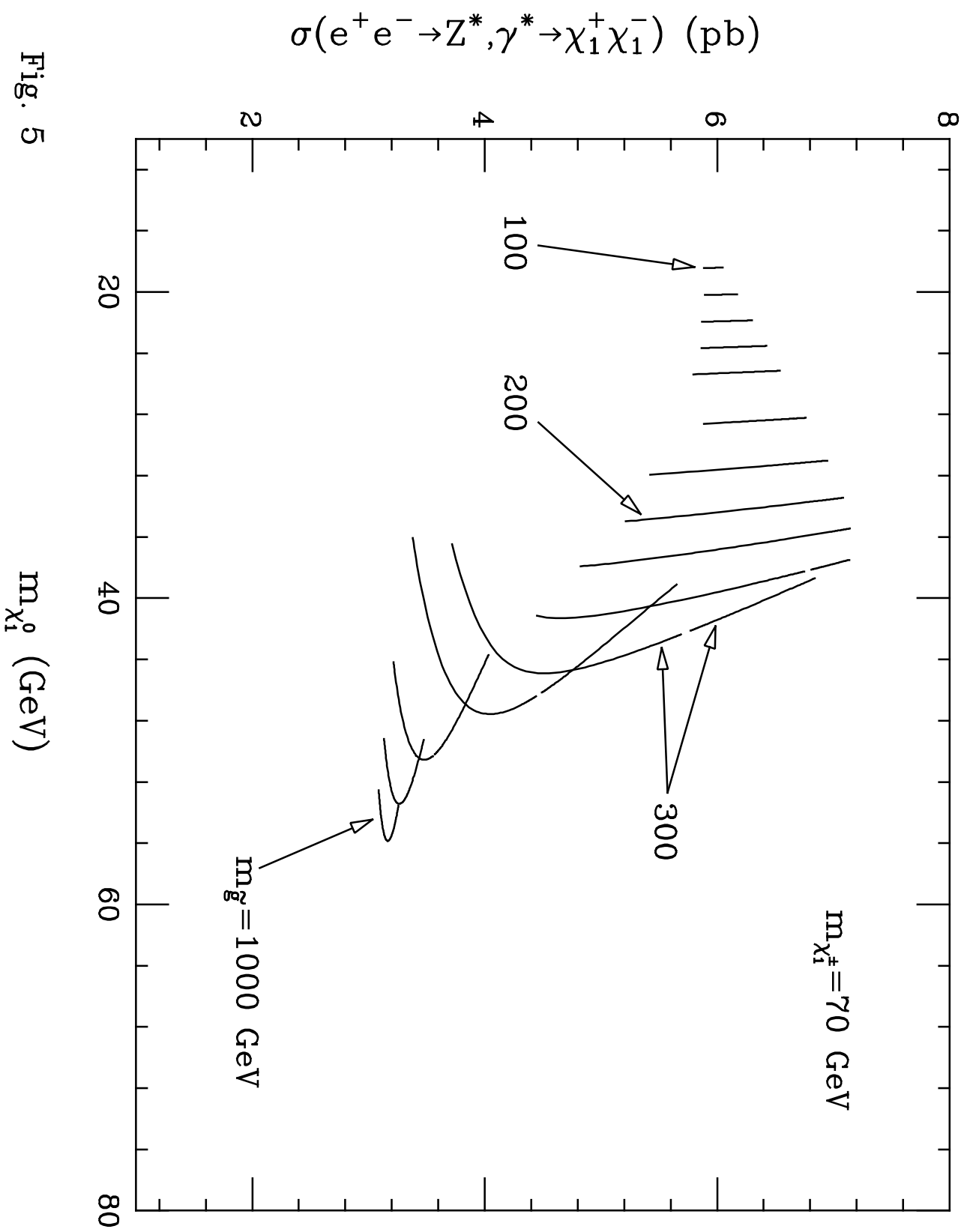


Fig. 5

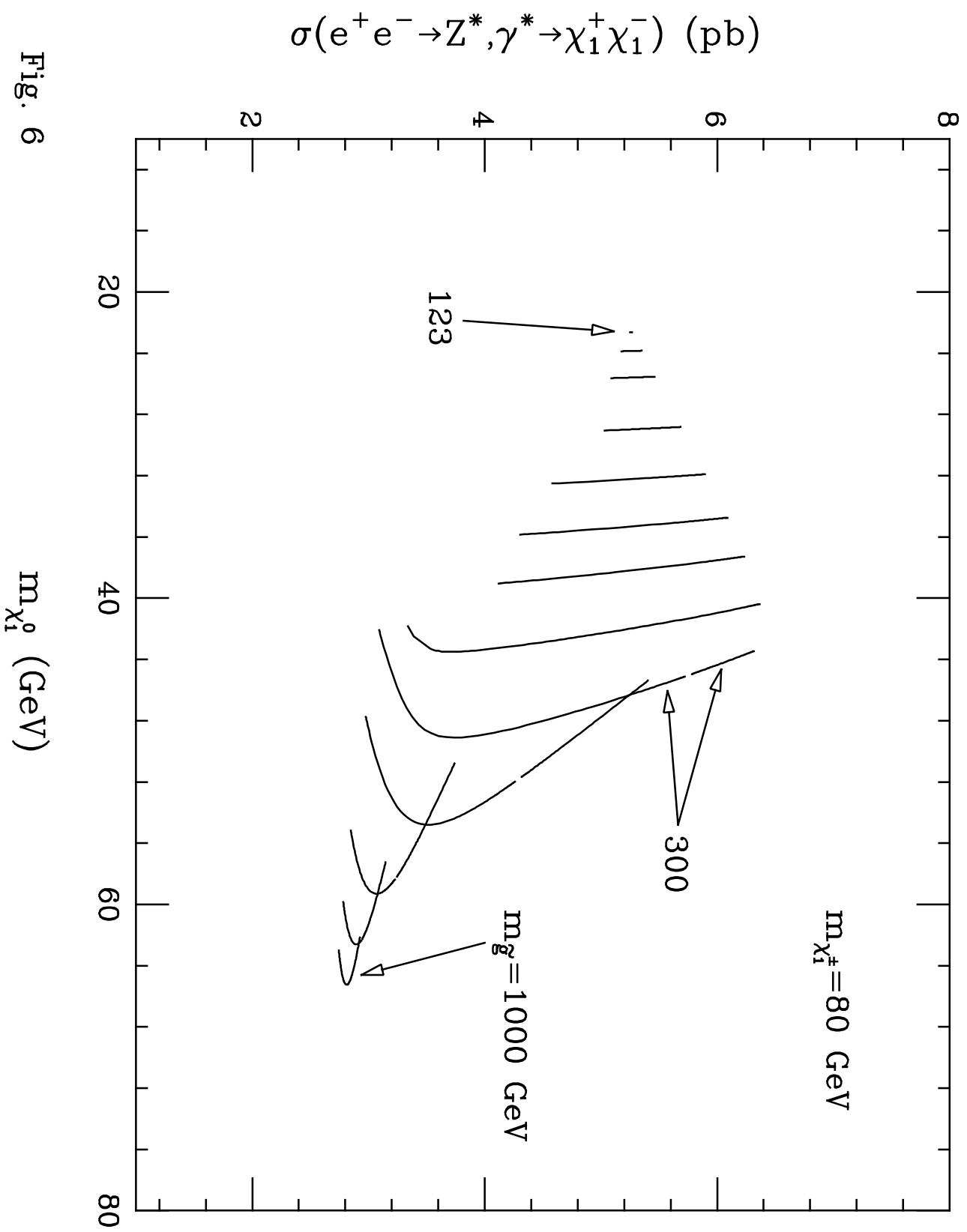


Fig. 6

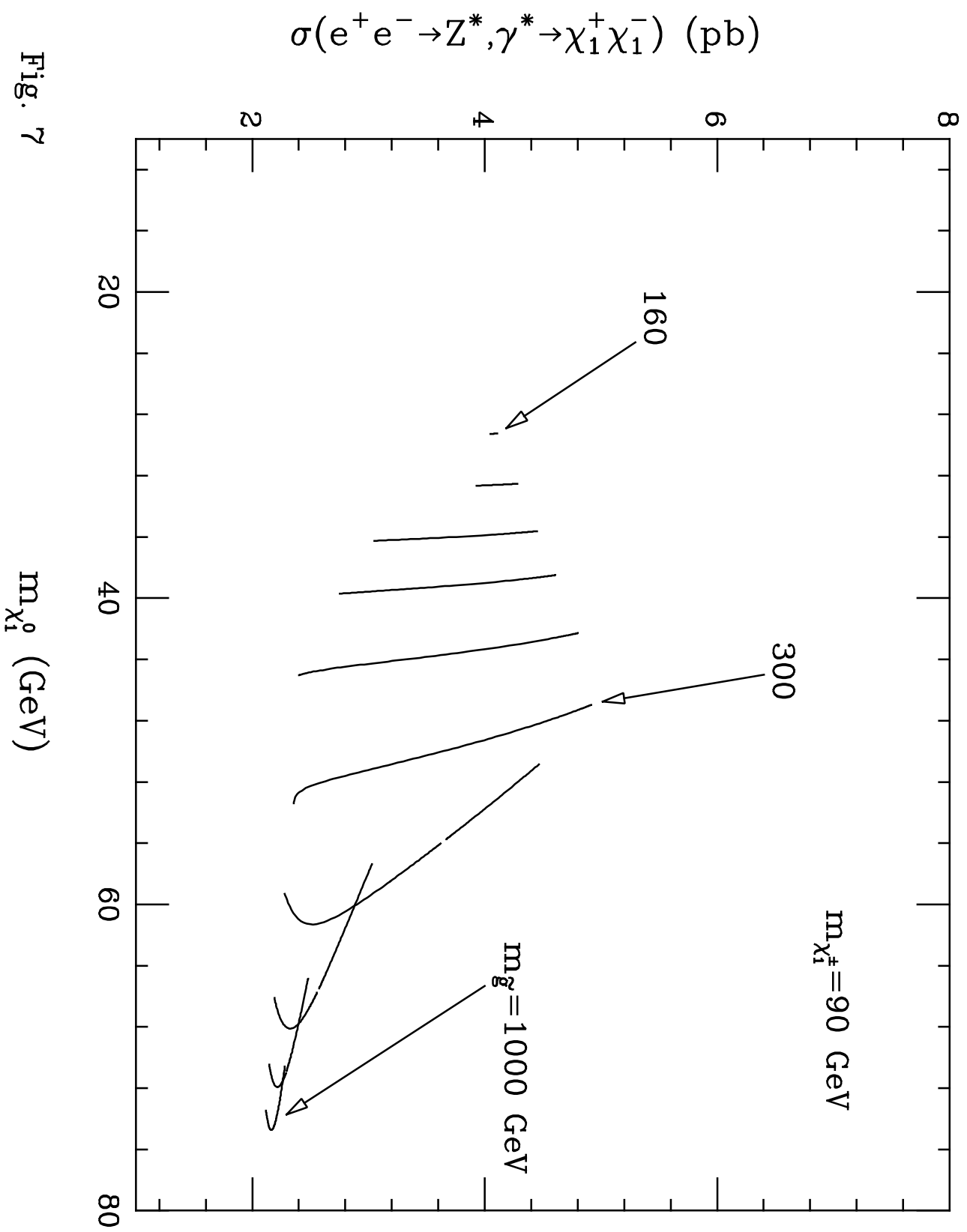


Fig. 7